Desalination and Water Treatment
www.deswater.com

doi: 10.1080/19443994.2013.838524

53 (2015) 469–474
January

Taylor & Francis
Taylor & Francis Group

Kinetic model of the ozone oxidation by-product bromate removal by nanoparticle zero iron

Yan Zhang[a,c,*], Hongyuan Liu[b], Runsheng Liu[a]

[a]*Department of Civil Engineering, Zhejiang University, Hangzhou, 310058, China*
Tel. +86 571 88206758/+1 780 8857515; Fax: +86 571 88208721; emails: zhangyan@zju.edu.cn, zhang11@ualberta.ca
[b]*College of Civil Engineering and Architecture, Zhejiang University of Technology, Hangzhou 310014, China*
[c]*Department of Civil & Environmental Engineering, University of Alberta, Edmonton, T6G 2W2, Canada*

Received 19 April 2013; Accepted 20 August 2013

ABSTRACT

Bromate formation during ozone oxidation process is becoming a particular concern because it is a carcinogenic compound. Reduction by zerovalent iron shows a potential technique for the removal of bromate from water. A series of batch experiments were carried out using nanoparticle zero iron. A tentative reaction mechanism and the kinetic model for bromate reduction were discussed. It was found that the efficiency of bromate removal was affected by the amount of iron, initial concentration of bromate, pH, and reaction temperature. Bromate removal was based on pseudo-first-order reaction kinetics, assuming an irreversible surface reaction to be the rate-controlling step. The apparent activation energy for bromate reduction, in the temperature range of 283–303 K, was found to be 23.2 kJ/mol.

Keywords: Bromate; Drinking Water; Dynamic; Nanoparticle zero iron (NZI); Ozone

1. Introduction

With the increasing application of ozone oxidation technology in drinking water treatment, the carcinogenicity of its by-product, bromate, which is formed during ozonation of bromide-containing waters, has drawn increased research [1]. Therefore, several techniques for the removal of bromate have been developed concurrently, including pH suppression [2], ammonia addition [3], granular activated carbon adsorption [4], ultraviolet irradiation [5], photocatalytic decomposition [6], ion exchange [7], biological remediation [8], and chemical reduction with Fe^{2+} or Fe^0 [9–11]. Considering the aforementioned measures, chemical reduction has been demonstrated as an effective method for bromate removal. In addition, it has been found that nanoparticle zero iron (NZI) has been used as a reductant for removing azo dye, nitrate, and perchlorate [12–14]. Furthermore, after its modification, NZI can be employed in water treatment or water remediation systems and effectively transported by water flow, because its particle size is smaller than the bulk zerovalent iron [15]. Therefore, chemical reduction by NZI seems to be a promising technology for bromate removal.

However, few studies have been systematically conducted in this aspect, especially in the dynamic model of bromate reduction by NZI. Therefore, the objective of the present work is to explain the mechanism and develop a dynamic model for bro-

---

*Corresponding author.

mate removal over NZI, so as to provide guidance for its further application.

2. Materials and methods

All chemical stock solutions were prepared from reagent-grade chemicals using doubled deionized water and stored at 4℃ unless otherwise specified.

2.1. NZI preparation and characterization

In this study, a series of NZIs were prepared by the liquid phase reduction method. It should be noted that when removing the NZI samples from the drying oven, the air valve should be connected to nitrogen gas to prevent NZI oxidation from atmospheric oxygen. In addition, the dried NZI samples should be transferred into an anaerobic chamber for future use.

Transmission electron microscope (TEM) was utilized to observe the shape and size of NZI under the conditions of an accelerating voltage of 100 kV. Moreover, field emission scanning electron microscopy (FESEM) was conducted to observe the surface morphology of the prepared NZI. The results can be seen in Fig. 1. It shows that most of the prepared iron particles were less than 100 nm in diameter. Furthermore, the aggregated nanoparticles could be also observed in the formation of chain-like structures, which might result from the magnetic property and large specific surface area of NZI samples.

X-ray diffraction pattern of NZI was also recorded by an X-ray diffractometer (X'Pert PRO, the Netherlands) with Cu Kα radiation in the 2θ range of 10–80˚ (scan power: 40 kV × 300 mA, step size: 0.0167˚ 2θ, step time: 10 s). It was found that the main reflection characteristic peak was recorded in 44.75˚ 2θ, which is consistent with the characteristic peak of Fe^0.

Furthermore, the Brunauer–Emmett–Teller (BET) surface area of the prepared NZI was determined by nitrogen adsorption with TriStar II 3020 surface area and porosity analyzer. The results show that the BET surface area was 20.98 m^2/g.

2.2. Batch experiments

The batch experiments were carried out in a 1,000 ml reactor under constant temperature and atmospheric pressure conditions. The solution temperature was controlled using an electric-heated thermostatic water bath. Prior to the experiments, a certain concentration of bromate solution was filled in the reactor and nitrogen gas was then introduced from the bottom of the reactor through a diffuser, in order to strip out dissolved and adsorbed oxygen. In addition, the pH value was determined by adding 0.1 mol/L NaOH or 0.1 mol/L HCl solution, and without buffer addition during the experimental period. Then a predetermined quantity of NZI was added to the reactor and suspended in the solution through stirring.

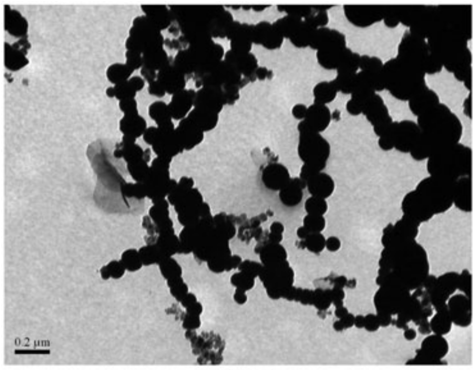

(a) TEM

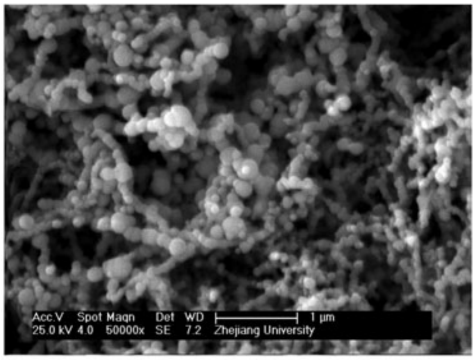

(b) FESEM

Fig. 1. TEM and FESEM images of prepared NZI.

Unless otherwise specified, the experiments were carried out under the amount of NZI, pH, dissolved oxygen, reaction temperature, mixing rate, and initial bromate concentration of 1 mg/L, 7.0, 0.04 mg/L, 293 K, 400 rpm, and 100 µg/L, respectively.

Samples were periodically taken from the suspension and analyzed for bromate, bromide, iron, and pH. Bromate and bromide were measured using a Dionex ICS-2000 ion chromatograph; the concentration of iron was determined using an ICE3500 atomic adsorption spectrophotometer, and the solution pH value was periodically monitored with an Orion 3 pH analyzer.

3. Results and discussion

3.1. Reaction mechanism

Fig. 2 shows the concentration profiles of bromate (measured as bromine), bromide, and total bromine (total bromine represents the sum of the current concentrations of bromate (measured as bromine and bromide) during the batch experimental period. It clearly illustrates that the concentration of bromate was quickly reduced within 20 min, while the concentration of bromide increased accordingly. Moreover, the concentration of the total bromine remained a constant value. The results demonstrate that NZI can effectively reduce bromate to bromide, and no intermediate product is found during the reaction period. The reduction reaction occurs on the surface of NZI and little or no bromate and bromide ions adsorbed on the NZI surface was found under the experimental conditions.

The equations of bromate reduced to bromide by NZI can be illustrated by the following:

$$BrO_3^- + 3Fe + 6H^+ \rightarrow Br^- + 3H_2O + 3Fe^{2+} \tag{1}$$

$$BrO_3^- + 3Fe + 3H_2O \rightarrow Br^- + 6OH^- + 3Fe^{2+} \tag{2}$$

While the experiments were carried out under acidic conditions, Fe^{2+} can be further oxidized to Fe^{3+}, as shown below:

$$BrO_3^- + 6Fe^{2+} + 6H^+ \rightarrow Br^- + 3H_2O + 6Fe^{3+} \tag{3}$$

3.2. Dynamic model

A series of experiments on the effect of the initial concentration of BrO_3^- on the bromate removal were carried out. The results can be seen in Fig. 3. It demonstrates that $\ln(c_0/c)$ (c_0 and c represent the initial and the current concentrations of bromate, respectively) has a clear linear relationship with the reaction time, that is to say, the reaction rate is independent of the current concentration of bromate. Furthermore, the reaction order is found to be approximately 1 under the experimental conditions. Such a linear relation between the bromate removal rate and the concentration of bromate follows a typical Langmuir–Hinshelwood function.

Bromate reduction reaction can be described by pseudo-first-order reaction kinetics, as shown below:

$$\frac{dc}{dt} = -k_{obs}c \tag{4}$$

$$\ln(c_0/c) = k_{obs}t \tag{5}$$

where c_0 and c are the same as above, and k_{obs} is the apparent rate constant, min^{-1}.

Fig. 4 illustrates the relationships between $\ln(c_0/c)$ and reaction time under different amounts of NZI. It shows that k_{obs} increased with the increasing amount of NZI. When the amount of NZI increased from 0.25 to 2 mg/L, k_{obs} improved from 0.019 to 0.32 min^{-1}. Moreover, Fig. 5 shows a strong linear relationship between k_{obs} and the amount of NZI. This can be explained that the rate-controlling step of bromate reduction by NZI is surface reaction. And NZI surface area increased with the increasing amount of NZI, thereby resulting in more contacting chance between bromate and NZI, thus the bromate reduction rate increased.

The effect of initial pH on the bromate reduction was also studied. It can be found that bromate reduction efficiency obviously declined as the pH value

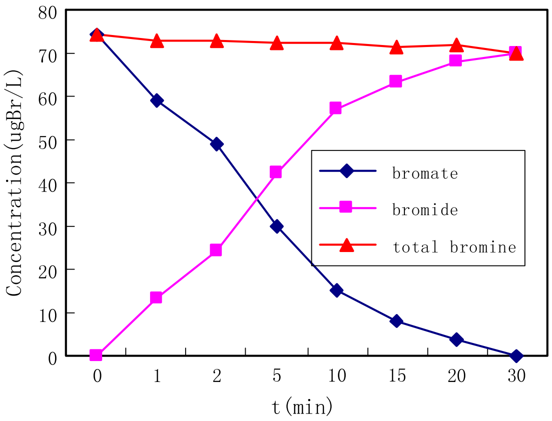

Fig. 2. Concentration profiles of bromate (measured as bromine), bromide and total bromine (NZI = 1 mg/L, pH = 7.0, **initial** BrO_3^- = 100 μg/L, temperature = 293 K, mixing rate = 400 rpm).

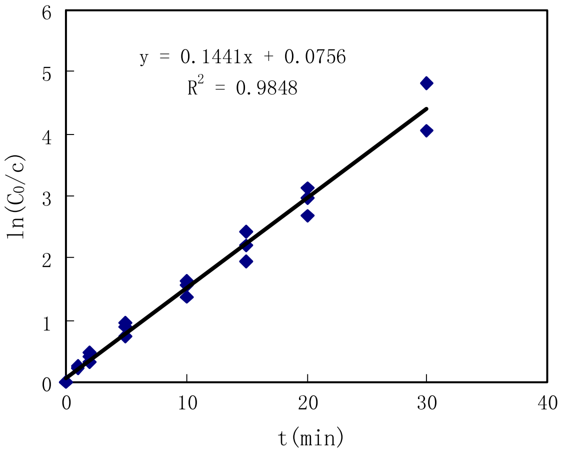

Fig. 3. Bromate reduction under various initial bromate concentrations (NZI = 1 mg/L, pH = 7.0, temperature = 293 K, mixing rate = 400 rpm).

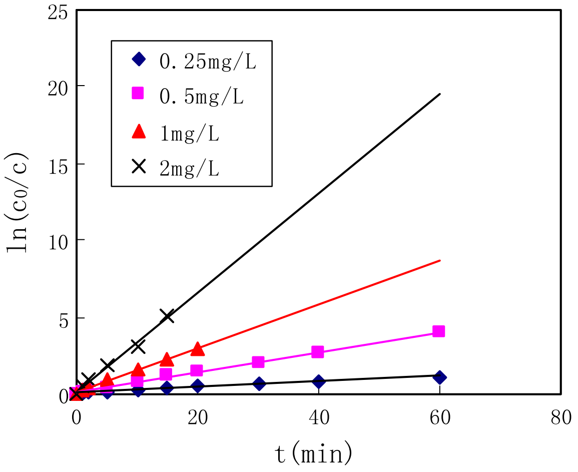

Fig. 4. Bromate reduction under the different amounts of NZI (pH = 7.0, initial BrO_3^- = 100 μg/L, temperature = 293 K, mixing rate = 400 rpm).

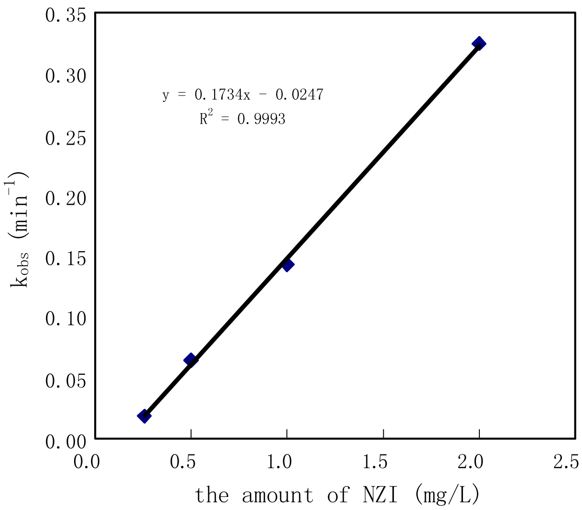

Fig. 5. The linear regression between k_{obs} and the amount of NZI (pH = 7.0, initial BrO_3^- = 100 μg/L, temperature = 293 K, mixing rate = 400 rpm).

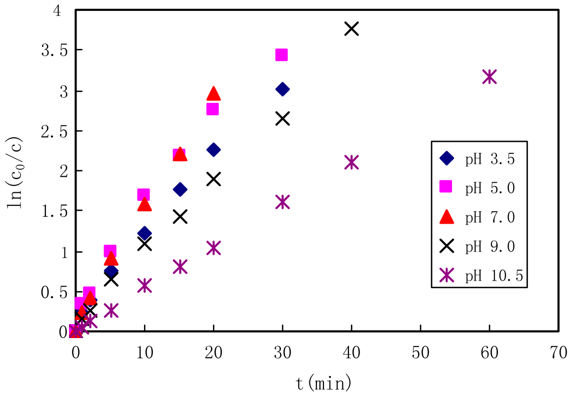

Fig. 6. Bromate reduction under the different initial pH value (NZI = 1 mg/L, initial BrO_3^- = 100 μg/L, temperature = 293 K, mixing rate = 400 rpm).

increased from 7.0 to 10.5. It can be explained that increasing the pH value means increasing the concentration of OH^-, and then iron hydroxide precipitation could be formed on NZI surface, which hindered bromate reduction.

Moreover, it can be found from Figs. 6 and 7 that bromate removal rate slightly improved when the pH value decreased from 7 to 5, and while the pH value continued to decrease to 3.5, the bromate removal rate did not increase, however, it showed a slight decrease. It can be explained that pH value had dual effect on bromate reduction under acidic conditions. First, when pH value decreased, the concentration of H^+ increased, which could accelerate the bromate removal according the reaction mechanism, as shown in Eqs. (1)–(3). On the other hand, when the pH value further decreased, the reaction between irons and H^+ enhanced, which would consume a certain amount of NZI. The effect on hindering bromate removal played a more important role than that on promoting when the pH value continuously decreased to 3.5, thereby bromate removal rate showed a slightly downward trend. Further analysis indicated that no significant effect of pH was observed on bromate reduction when the pH value was in the range of 3.5–7.0 under the experimental conditions, because of the combined effect of hindering and promoting on bromate removal.

The influence of reaction temperature on bromate reduction over NZI was investigated between 283 and 303 K. The results were displayed in Fig. 8 and Table 1.

It can be found from Fig. 8 that the apparent rate constant (k_{obs}) increased as temperature rose. The k_{obs} improved from 0.10 to 0.19 min^{-1} with the temperature rose from 283 to 303 K. Using Arrhenius equation [16], the apparent activation energy for bromate reduction can be calculated from the change of temperature and apparent rate constant:

$$\ln k_{obs} = -\frac{E}{RT} + \text{const} \tag{6}$$

(where k_{obs} is the apparent rate constant, min^{-1}; E is the apparent activation energy, kJ/mol; T is the reaction temperature, K; and R is the universal gas constant, $R = 8.314$ J/(mol.K)).

Under the experimental conditions, E value was equal to 23.2 kJ/mol. The low value of apparent activation energy obtained in this work further confirmed

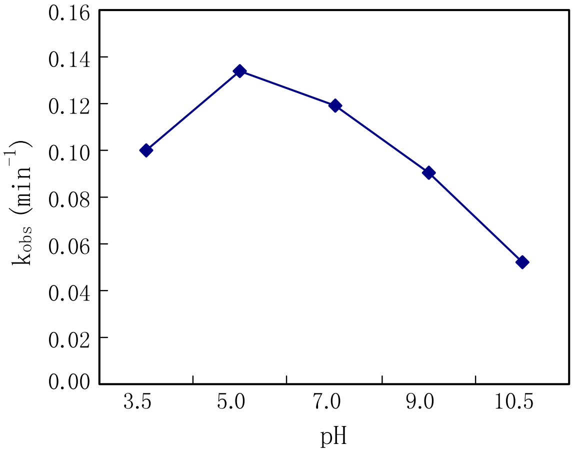

Fig. 7. The relationship curve between k_{obs} and initial pH value (NZI = 1 mg/L, initial BrO_3^- = 100 µg/L, temperature = 293 K, mixing rate = 400 rpm).

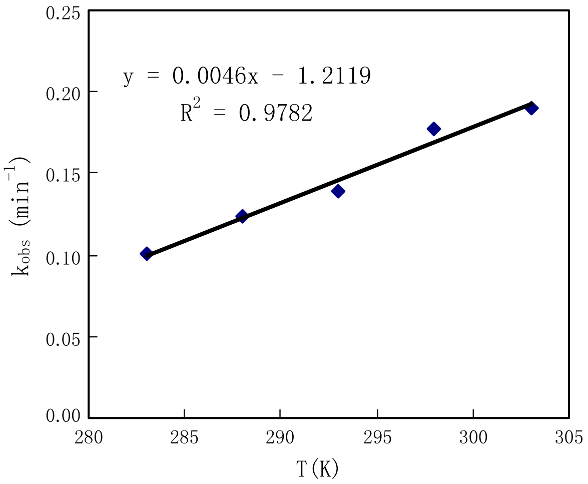

Fig. 8. The linear regression between k_{obs} and the reaction temperature (NZI = 1 mg/L, initial BrO_3^- = 100 µg/L, pH = 7.0, mixing rate = 400 rpm).

Table 1
k_{obs} and R^2 under different reaction temperature

Reaction condition		k_{obs} (min^{-1})	R^2
T (K)	283	0.10	0.9927
	288	0.12	0.9977
	293	0.14	0.9972
	298	0.18	0.9882
	303	0.19	0.9676

that the bromate reduction by NZI showed an effective technique and followed a surface-controlled reaction [17].

4. Conclusions

In this paper, reaction mechanism and the dynamic model for bromate reduction by NZI were discussed. It was found that the bromate reaction could be described by pseudo-first-order reaction kinetics and followed surface-controlled reaction. Bromate removal rate increased with the increasing amount of nanoparticles iron and reaction temperature. The pH value had dual effect on bromate reduction, and acidic conditions were beneficial in improving the bromate removal efficiency. The low value of apparent activation energy obtained in this work confirmed that the bromate reduction by NZI showed a promising technique for bromate removal from water.

Acknowledgments

This work was supported by National Natural Science Foundation of China (No. 51108407), the Fundamental Research Funds for the Central Universities (No. 2011FZA4022), and Zhejiang Innovation Teams Funds (No. 2010R50037).

References

[1] U. von Gunten, Ozonation of drinking water. Part II: Disinfection and by-product formation in presence of bromide, iodide or chlorine, Water Res. 37 (2003) 1469–1487.
[2] U. Pinkernell, U. von Gunten, Bromate minimization during ozonation: Mechanistic considerations, Environ. Sci. Technol. 35 (2001) 2525–2531.
[3] M.D. Williams, B.M. Coffey, S.W. Krasner, Evaluation of pH and ammonia for controlling bromate during cryptosporidium disinfection, J. Am. Water Works Assn. 95 (2003) 82–93.
[4] W. Huang, Y. Cheng, Effect of characteristics of activated carbon on removal of bromate, Sep. Purif. Technol. 59 (2008) 101–107.
[5] N.H. Phillip, E. Gürten, V. Diyamandolu, Transformation of bromine species during decomposition of bromate under UV light from low pressure mercury vapor lamps, Ozone-Sci. Eng. 28 (2006) 217–228.
[6] A. Mills, A. Belghazi, D. Rodman, Bromate removal from drinking water by semiconductor photocatalysis, Water Res. 30 (1996) 1973–1978.
[7] J.A. Wiśniewski, M. Kabsch-Korbutowicz, Bromate removal in the ion-exchange process, Desalination 261 (2010) 197–201.
[8] W.A.M. Hijnen, R. Jong, D. van der Kooij, Bromate removal in a denitrifying bioreactor used in water treatment, Water Res. 33 (1999) 1049–1053.
[9] G. Gordon, R.D. Gauw, G.L. Emmert, B.D. Walters, B. Bubnis, Chemical reduction methods for bromate ion removal, J. Am. Water Works Assn. 94 (2002) 91–98.
[10] P. Westerhoff, Reduction of nitrate, bromate, and chlorate by zero valent iron, J. Environ. Eng. 129 (2003) 10–16.
[11] L. Xie, C. Shang, The effects of operational parameters and common anions on the reactivity of zero-valent iron in bromate reduction, Chemosphere 66 (2007) 1652–1659.
[12] J. Cao, D. Elliott, W. Zhang, Perchlorate reduction by nanoscale iron particles, J. Nanopart. Res. 7 (2005) 499–506.
[13] H.Y. Shu, M.C. Chang, H.H. Yu, W.H. Chen, Reduction of an azo dye acid black 24 solution using synthesized nanoscale zerovalent iron particles, J. Colloid Interface Sci. 314 (2007) 89–97.

[14] Z. Jiang, L. Lu, W. Zhang, Q. Du, B. Pan, L. Yang, Q. Zhang, Nitrate reduction using nanosized zero-valent iron supported by polystyrene resins: Role of surface functional groups, Water Res. 45 (2011) 2191–2198.

[15] S.M. Ponder, J.G. Darab, T.E. Mallouk, Remediation of Cr(VI) and Pb(II) aqueous solutions using supported, nanoscale zerovalent iron, Environ. Sci. Technol. 34 (2000) 2564–2569.

[16] C. Su, R.W. Puls, Kinetics of trichloroethene reduction by zerovalent iron and tin: Pretreatment effect, apparent activation energy, and intermediate products, Environ. Sci. Technol. 33 (1999) 163–168.

[17] B. Deng, D.R. Burris, T.J. Campbell, Reduction of vinyl chloride in metallic iron-water systems, Environ. Sci. Technol. 33 (1999) 2651–2656.